IEEE Copyright Notice

Cooperative μUAV-UGV autonomous indoor surveillance

Martin Saska, Tomáš Krajník, Libor Přeučil,
Department of Cybernetics, Faculty of Electrical Engineering, Czech Technical University in Prague
{saska,tkrajnik,preucil}@labe.felk.cvut.cz

***Index Terms*—UAV, surveillance, autonomous navigation**

***Abstract*—In this paper, we present a heterogenous UGV-UAV system cooperatively solving tasks of periodical surveillance in indoor environments. In the proposed scenario, the UGV is equipped with an interactive helipad and it acts as a carrier of the UAV. The UAV is a light-weight quadro-rotor helicopter equipped with two cameras, which are used to inspect locations inaccessible for the UGV. The paper is focused on the most crucial aspects of the proposed UAV-UGV periodical surveillance that are visual navigation, localization and autonomous landing that need to be done periodically. We propose two concepts of mobile helipads employed for correction of imprecise landing of the UAV. Beside the description of the visual navigation, relative localization and both helipads, a study of landing performance is provided. The performance of the complex system is proven by an experiment of autonomous periodical surveillance in a changing environment with presence of people.**

I. Introduction

The character of surveillance and inspection tasks predestinates extensive utilization of autonomous mobile robots. The robots are able to perform repetitive, tiresome tasks without losing concentration. They can be deployed in inhospitable workplaces and they can carry sensors exceeding human perception. Even now, mobile robots are employed for periodical patrolling along pre-learnt paths and for inspection and search&rescue missions in dangerous environments [1]. Although, one can find examples of utilization of Unmanned Ground Vehicles (UGV) [2] as well as Unmanned Aerial Vehicles (UAV) [3], the ability to perform inspection tasks of both these systems is limited. The μUAVs (usually quadro-rotor helicopters), which are able of indoor operation, are constrained by their short operational time (tens of minutes) and by their low payload (hundreds of grams). Contrariwise, the UGVs can operate for extended periods of time and can carry substantial payloads, but their movement is limited by obstacles and terrain traversability.

In this paper, we present a research aiming towards a heterogenous system that is able to overcome the above mentioned limitations. The main idea is to couple two robots, one UGV and one μUAV into a heterogenous closely cooperating team. We propose a scenario, where the UGV is equipped with all necessary sensors for the task of surveillance and with a high-capacity power source. Besides, the ground robot is equipped with a helipad and it acts as a carrier of a μUAV. The μUAV is a cheap quadro-rotor helicopter [4] equipped with two cameras, which are used to inspect locations inaccessible for the ground robot.

Let us describe the cooperation of members of such a team during a scenario of periodical surveillance, which is our target application. The objective of the robotic team is to periodically visit a set of places of interest, which have been pre-selected by security experts. During the mission, the UGV follows a pre-planned path and sequentially scans the places of interest by its sensors. Once a place of interest cannot be reached by the UGV due to environment constraints, the μUAV is launched from the UGV helipad to perform the inspection. Since the UGV position in the moment of takeoff is known, we use a relative localization method similar to the one described in papers [5] [6] to determine its absolute position. Using a relative localization to the UGV positioned in the known take-off location, the desired place of interest is autonomously reached and scanned by the quadro-rotor μUAV. Once the image of the inspected area is captured, the μUAV returns back to the helipad attached on the ground robot and the heterogenous team continues towards the next place of interest. Such a sequence consisting of autonomous taking off, flying to the desired location, scanning the place of interest, returning back to the mobile base and landing on the helipad can be repeated several times during one round of the patrolling trip.

This approach enables to use the limited operational time of μUAVs efficiently. The μUAV begins its task as close to places of interest as possible and it visits only the places inaccessible by the UGV. Since the μUAV flight time is short and it keeps close to the UGV, its position estimation can be based on combination of dead reckoning and visual tracking. The simplicity of relative localization between the μUAV and UGV allows to use a cheap μUAV without heavy sensory and computational equipment, which would be necessary for advanced localization algorithms. Moreover, the μUAV battery can be replenished between two flights from the energy source of UGV using a recharging system installed on the helipad.

This paper is focused on the most crucial aspects of the proposed μUAV-UGV periodical surveillance that have been identified during preliminary experiments. In the first part of the paper, systems of visual navigation and localization are described. The second part of the paper deals with technical aspects of the autonomous landing and taking-off that need to be done periodically. Beside technical descriptions and comparison of developed landing systems, results of an experiment of cooperative μUAV-UGV autonomous indoor surveillance is provided to verify the usability of the entire system.

II. Visual navigation and localization

The ground robot is navigated between the predefined waypoints using a visual navigation system [7]. For the μUAV autonomous flight and landing, a control algorithm based on visual relative localization from the UGV was developed [4]. The method either uses the bottom UAV camera to localize a pattern on the helipad or estimates the UAV position from accelerometer, gyro and optical flow measurements. The UGV navigation method is based on a "map and replay" technique. A security specialist guides the UGV along the required path and designates the places to be inspected. At these places, either the UGV takes a snapshot of the environment or the UAV takes off and performs inspection with its cameras.

A. UGV navigation

The UGV navigation is based on monocular vision and odometry. It works in two steps: mapping and navigation. In the mapping phase, the robot is guided by the security specialist along a path consisting of straight-line segments. During this guided tour, the robot uses the GPU version [8] of the Speeded Up Robust Features (SURF) [9] algorithm to extract salient features from its onboard camera image. These features are tracked and their image coordinates and descriptors are recorded. Once the mapping is finished, the robot can autonomously traverse the learned path. Optionally, the gathered map quality might me be enhanced by methods [10], [11].

1) Mapping phase: The robot is driven through the environment by a human operator in a turn-move manner and creates a map. The security specialist can either stop the robot and change its orientation or let the robot move forwards with a constant speed. The resulting map has a form of a sequence of straight segments.

Each segment is described by the initial robot orientation α given by robot compass, the segment length s measured by odometry, and the landmark set $\mathbf{L}$. The set $\mathbf{L}$ consists of salient features detected in images captured by the robots forward looking camera by the aforementioned SURF method. Each landmark $\mathbf{l} \in \mathbf{L}$ is described by its image coordinates and by the robot distance from the segment start when the landmark tracking was initiated and finished. This information is then utilized in the navigation phase.

The landmark tracking is performed as follows. The mapping algorithm maintains three sets of landmarks: a set of tracked landmarks $\mathbf{T}$, a set of currently detected landmarks $\mathbf{S}$ and a set of saved landmarks $\mathbf{L}$. Each time a picture is processed by the SURF algorithm, correspondences are established between the sets $\mathbf{S}$ and $\mathbf{T}$. The descriptions (image coordinates and the current robot position) of the landmarks in the set $\mathbf{T}$ are then updated based on the data of the set $\mathbf{S}$. The landmarks in the set $\mathbf{T}$, which have not been matched, are added to the set $\mathbf{L}$. Similarly, the unmatched landmarks in $\mathbf{S}$ are added to the set $\mathbf{T}$. When the mapping is completed, each feature in the set $\mathbf{L}$ is described by its SURF vector, image coordinates and values of the robot odometric counter in instants of its first and last detection.

2) Navigation phase: During the autonomous navigation, the robot maintains constant forward speed until its odometry indicates that its distance from the segment start is equal to the segment length. The robot steering speed is calculated from the positions of previously mapped and the currently detected landmarks. First, a relevant set of landmarks $\mathbf{U}$ is retrieved from the set of mapped landmarks $\mathbf{L}$. The set $\mathbf{U}$ contains landmarks that were detected in the mapping phase at the same robot distance from the segment start. For each landmarks in the set $\mathbf{U}$, the best matching landmark in the set $\mathbf{S}$ (landmarks detected in the current image) is found in the similar way as in the mapping phase. A difference in horizontal image coordinates of the paired landmarks is then computed and stored in a set $\mathbf{H}$. A histogram of the values in the set $\mathbf{H}$ is then created and the bin with the largest amount of landmarks is used to compute the robot steering speed ω. This simple way of visual servoing efficiently compensates robot lateral position deviation from the learned path. A typical view from the UGV camera together with detected features, established pairs and position difference histogram is shown at Figure 1.

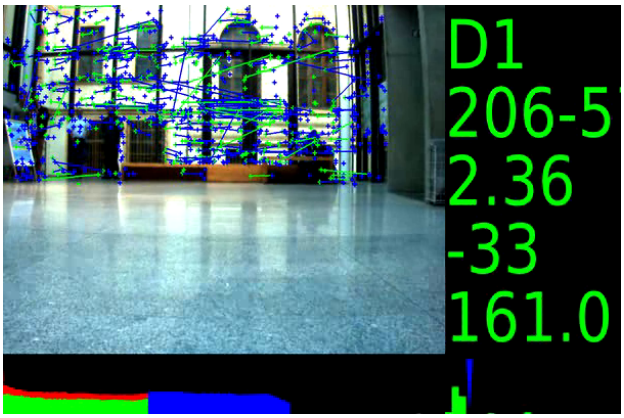

Fig. 1. Robot GUI during autonomous navigation

B. UAV localization

The UAV localization is based on two different methods. The first method is based on the drone dead-reckoning system, which estimates drone speed based on the optical flow in the image of its bottom camera [12]. These speeds are simply integrated to get an estimate of the drone position.

The second method searches the UAV bottom camera image for colored patterns placed on the heliport. The pattern is used to define the origin and orientation of the coordinate system of the drone. Each pattern is composed of two colored rectangles of known size, color and position. The image processing algorithm first searches for continuous regions of a given color and computes their centers and size. Then the method selects two largest regions of the given color and computes drone altitude from the distance of their centers. The drone heading is calculated from the relative position of both centers. After that, the drone position is computed from its pitch, roll and image coordinates of the pattern center.

The heliport contains two patterns with different colors. The larger pattern is used in normal operation and is detectable up to a six meter altitude. The smaller colored pattern is used when the drone altitude is so low, that the bottom camera field of view is insufficient to contain the complete larger pattern. This is particularly useful during the landing maneuver. A view of the active heliport, with the large (red) and the small (green) pattern, is on Figure 2.

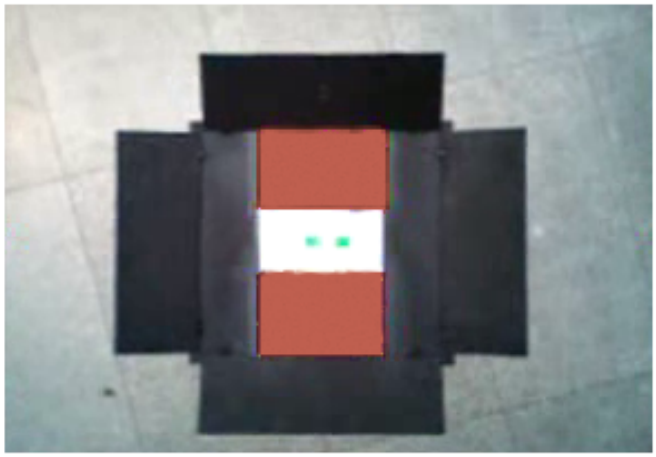

Fig. 2. Heliport from the UAV bottom camera view.

The disadvantage of using colored landing patterns is the need of color calibration and a potential danger of false-positive pattern misdetection. To overcome this issue, we are testing a black and white pattern similar to the ones presented in [5] and [6]. However, the black and white pattern detection algorithm sometimes fails due motion blur in the bottom camera image. Therefore, the μUAV has to perform slower maneuvers than in the case of colored pattern detection method.

The UAV uses the heliport pattern for localization whenever it is detected in the bottom camera image. When the heliport is out of view, the drone has to rely on its dead-reckoning. The dead reckoning precision is sufficient, because in our application scenario, the UAV leaves the heliport out of its view only for a few seconds. Such a time period is short enough to prevent the dead reckoning error to accumulate.

C. UAV navigation

Since we have the UAV localized with sufficient precision, its navigation can be based on a relatively simple position controller. Thanks to the fact, that the AR Drone interface allows to set the quadrotor angles and vertical speed rather than setting the individual turbine speeds, the position controller can be decoupled to four independent controllers. The yaw controller is the simplest one, see Figure 3 - it sets the μUAV turning speed to keep it aligned with the coordinate system defined by the UGV orientation. The altitude controller takes into account the difference between desired and measured altitude and sets the drone vertical speed, see Figure 4. The drone is aligned to the UGV coordinate frame, and therefore,

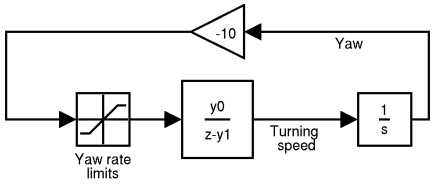

Fig. 3. Structure of the yaw controller.

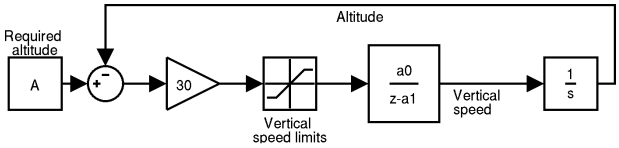

Fig. 4. Structure of the altitude controller.

the x coordinate of the drone is controlled by its pitch and its y coordinate is controlled by the drone roll. Since the drone is symmetrical, its pitch and roll controllers have identical structure, see Figure 5. So, the pitch controller takes into account the quadrotor actual pitch, forward speed and the target x coordinate and computes the pitch command. The roll controller computes roll from the actual roll, sideward speed and relative y coordinate of the target.

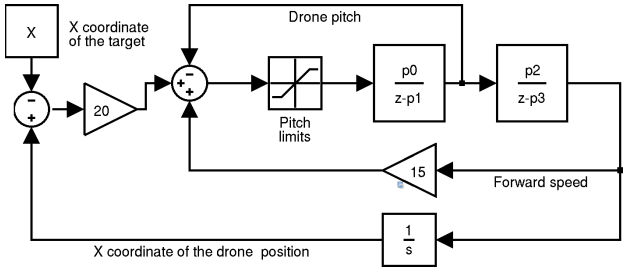

Fig. 5. Structure of the pitch (and roll) controller.

The navigation can be divided in four phases: takeoff, flight to the inspection point, return to the heliport and landing. So let us assume, that the UGV arrived at the takeoff location and the drone is supposed to reach coordinates (x, y, z) in the heliport coordinate frame. During takeoff, the drone keeps itself directly above the heliport, holds its yaw aligned with the robot orientation and gradually increases its altitude. Once the desired altitude is reached, the values of x, y are fed to the pitch and roll controllers and the UAV starts to move towards the destination. When the destination is reached, the drone takes several snapshots with its cameras, then sets the desired position to $(0, 0, z)$ and moves back. Once it detects the heliport pattern, it locks its position directly above heliport center and starts to gradually decrease its altitude. When the drone altitude is below 0.6 m, the heliport detection method is switched to detect the color of the smaller pattern. Once the altitude drops below 0.3 m, the drone switches off its propellers and lands.

III. Concept of active and passive helipads

Although the visual localization and UAV control during the landing phase are relatively precise, a deviation of UAV position on the helipad can occur due to unpredictable air turbulences. The light-weight helicopters are intensively effected by inhomogeneities of air-flow along edges of the mobile helipad as was identified in numerous experiments. Precise positioning on the helipad attached on a UGV is crucial for the recharging of UAV, where the charging pins need to be locked to relatively small sockets, and for repeated landing, where the deviation from the required position on the helipad could cause break-off of the relative localization in the take-off phase. Even a small deviation of inclination of the μUAV on the helipad can cause the quadcopter to lose visual contact with the UGV during the takeoff maneuver, which might cause a fatal disconnection of the heterogeneous system.

Two different prototypes of mobile helipads have been designed, constructed and experimentally verified to decrease error in position after the landing on UGVs (see Fig. 6 for their pictures and schemes). Both concepts can be mounted on the top of the P3AT robot (or a platform of similar size) and they can correct the landing position of the AR-Drone [13] quadcopter. The first helipad prototype does not contain any movable components and corrects the position of the μUAV in the center of helipad passively. This, so-called passive helipad, is constructed with four square tapered holes with their vertices located in the desired positions of landing feet of the micro-helicopter. Due to the descent of the hollow pyramids, the position error of UAV is significantly diminished in the landing phase. During the landing maneuver the μUAV landing gear interlocks into the cones, causing the drone to finish the flight in a clearly specified position.

The second landing platform actively cooperates with the μUAV during the landing procedure. This, so called active helipad, is based on four folding sideboards driven by a servomechanism. Using these plates, the active helipad corrects imprecise landing position of the μUAV and adjusts the quadrotor helicopter into the desired position and orientation. The sideboards are outspread during the UAV landing, which temporarily enlarges surface of the helipad. Once the successful landing is detected by the UAV-UGV control system, the helicopter is actively pushed to the center of the helipad by the sideboards.

For the design of experimental prototype, we have chosen servos Hi-tech (type: HS-485 HB) that are mounted to lower side of the base. The servos are controlled by PWM signal with frequency 50 Hz and pulse width ranges from 600s to 2400s. The sideboards are opened completely if the pulse width is 600s and closed if the pulse width is 2400s. The sideboards are controlled by two channels of PWM signals. One channel controls two adjacent servos. This approach has been experimentally identified as the appropriate way to relieve the helicopter from blockages. For generating the waveforms, we have employed a micro-controller AT-Mega8, which generates two PWM signal with frequency of 50Hz and the required pulse widths.

A large set of experimental testing and analyses have been performed to determine characteristics of both devices. The experimental set includes none-flight experiments to verify theoretically computed operational space of heliports as well as a sequence of repeated landing and take-off with introduced additional disturbances in position determination to show robustness and precision of the system. Examples of the experimental results are presented in Fig. 8. In the experiment, AR-Drone fuselage was placed on the helipad in random positions, which were measured. The heading of the fuselage is depicted in Fig. 8(a) and position of the helicopter within the frame of the helipad is depicted in Fig. 8(b). In the next step, the correction procedure was activated and the new position of the helicopter was again measured (see corrected position of the UAV center in Fig. 8(c) and its orientation in Fig. 8(d)). The maximum error between the desired position of the center of helicopter and its position after the correction was 21 mm, which is sufficient for the repeated take-off as well as for possible battery recharge.

For the passive helipad, such a visualization of results is not necessary, since the required final position (determined by the positions of the cones) was achieved whenever the landing legs are inside the hollow pyramids during the landing. The operational space of the passive helipad can be therefore determined precisely by the size of bases of the pyramids and size of the AR-Drone. Such analytically computed work space, denoted in Fig 7, has been verified via numerous experiments. In Fig. 7, one can see a visualization of the operational spaces of both concepts for comparison. The green contours highlight edges of both types of helipads (their size was equivalent for verification and comparison) and position of the the hollow pyramids in case of the passive approach. One can see, that the passive helipad is sensitive to deviations from the desired quadrotor heading during the landing. This effect could be reduced using cylindrical cones in case of the passive helipad and a circular protecting hull of AR-Drone in case of the active helipad.

At the end of this subsection let us compare the proposed approaches enabling long term cooperation of the AR-Drone platform with unmanned ground vehicles. The passive system profits from the lack of moving parts, which may be source of potential failures. Secondly, it can be used with the AR-Drone outdoor shell, which is not equipped with the hull protecting the propellers that is needed for landing on the active helipad. Contrariwise, the active helipad takes benefit of larger operational space at equal outer dimensions. Besides, the closed sideboards protect the UAV against sliding out of the helipad surface during UGV movement in a rough terrain. The concept of active helipad enables utilization of its flat surface, which is important for placement of patches needed for relative localization of the UAV. And finally, the helicopter does not need to be equipped with an extension of landing feet, as it is with the passive helipad. This extension, which depends on the depth of the tapered holes, decreases stability of the UAV if landing outside the helipad.

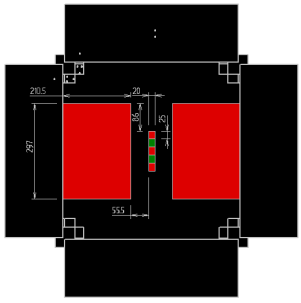

(a) Scheme of the active helipad.

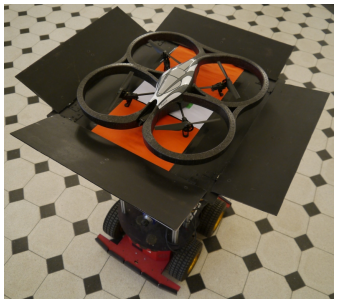

(b) Picture of the active helipad mounted on the Pioneer robot.

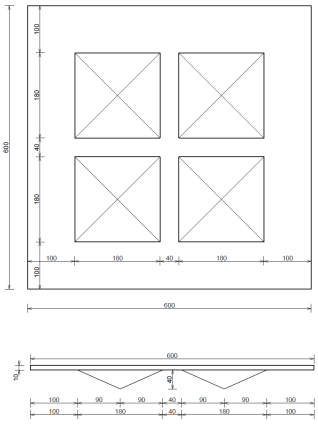

(c) Scheme of the passive helipad.

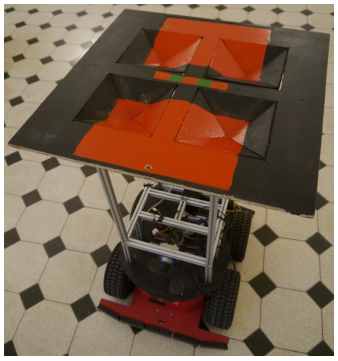

(d) Picture of the passive helipad mounted on the Pioneer robot.

Fig. 6. Description of both concepts of the mobile helipad.

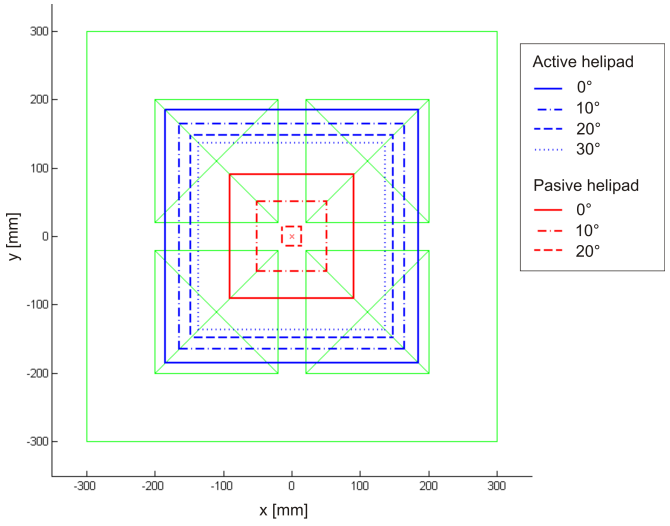

Fig. 7. Comparison of the workspace of both helipads with equal outer dimensions. The red (resp. blue) squares enclose the set of positions of UAV centres, for which a proper function of the passive (resp. active) system can be guaranteed. These borders have been identified by a sequence of experiments with different deviation from the desired heading. For both helipads the workspace is determined for different error in UAV heading regarding the orientation of the UGV.

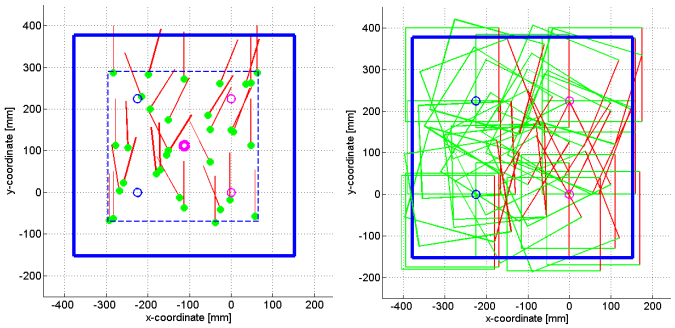

(a) Measured orientations of the AR-Drone after the landing.

(b) Measured positions of the AR-Drone after the landing.

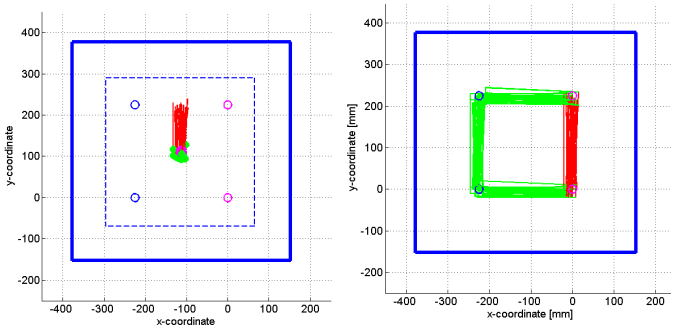

(c) Measured orientations of the AR-Drone after the correction by the sideboards.

(d) Measured positions of the AR-Drone after the correction by the sideboards.

Fig. 8. Results of the experiments with the dynamic helipad. The landing error was artificially increased to be able to identify performance of the helipad in its complete operational area.

IV. Experimental Deployment of the Entire System

The performance of the complete system is demonstrated by an experiment of periodical surveillance in an indoor environment (see snapshots from the experiment in Fig. 9 and a complete movie in [14]. In accordance with requirements of periodical surveillance as given above, a set of places of interest that need to be checked was identified and the UGV has been taught the required path by an expert. The places of interest are denoted for demonstration purposes with a picture card. These cards should be visible by the bottom camera of AR-Drone during its flyover. To verify the concept of direct cooperation of μUAVs and UGVs, all the places of interest were inaccessible by the mobile robot and a top view from the helicopter was necessary.

During the experiment, the P3AT robot carrying the AR-Drone on its active helipad is following the predefined path to the first take-off location. This movement is guided by the SURFNav [7] algorithm using the monocular camera of the robot. This approach is robust to changes in environment and therefore the learnt path for the surveillance does not need to be updated before each deployment of the system. Once the take-off location is reached, the UAV is launched to observe the place of interest, which is inaccessible by the mobile robot. During this task, its bottom camera is used for the relative localization with respect of the color patch on the

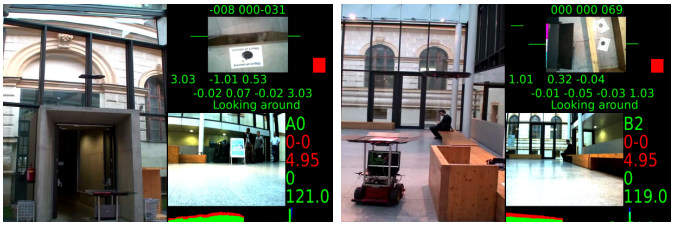

(a) The 1st object of interest is detected.

(b) The 2nd object of interest is detected.

(c) The UGV navigates towards the next take-off location.

(d) The active helipad is reopened and the μUAV is launched.

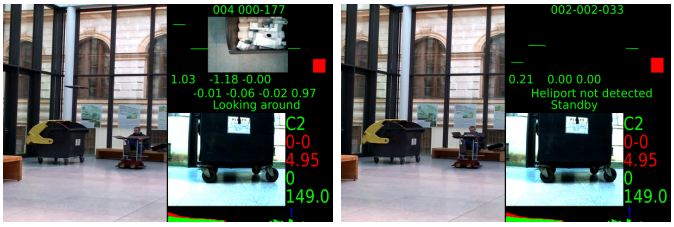

(e) The 3rd object of interest detected.

(f) The μUAV is positioned into the center of the helipad.

(g) The UGV is navigated towards the next take-off location.

(h) The 1st place re-visited in the 2nd round of the periodical surveillance.

Fig. 9. Snapshots from the hardware experiment of cooperative μUAV-UGV autonomous indoor surveillance.

helipad. In the part of the mission, where the patch is not visible by the camera, a dead-reckoning based on on-board sensors is employed. During the landing, the color patch is again used as a control feedback. After landing, the position of UAV is corrected by the active helipad and the helicopter is prepared for the next mission. Such a sequence is repeated for the next places of interest as shown in the sequence of snapshots in Fig. 9. Once all places of interest are observed, the surveillance round is repeated again. The total time of autonomous inspection is limited by the battery capacity of the ground robot.

V. Conclusion

In this paper, we presented enabling technologies for a heterogenous UGV-UAV system cooperatively solving task of periodical surveillance in indoor environments. Beside a method of relative navigation necessary for the direct cooperation between the ground and aerial robots, we have shown two approaches of mobile docking stations making the deployed team more compact and increasing its operational time and performance. In numerical flight and non-flight experiments, it was identified that the passive landing system provides cheap, robust and more reliable solution suited for industrial applications. Contrariwise, the active helipad offers better performance due to its larger operational space with the equivalent size and it provides additional protection of UAV during its carrying by the ground robot. These factors predestinate utilization of the active concept for inhospitable environment of search and rescue applications and for tasks of surveillance, where one can expect higher position error during landing due to wind, changing illumination conditions or other factors.

Acknowledgment

This work is supported by European Union under the grant Symbrion-Enlarged no. 216342, by GAČR under the grant no. P103-12/P756 and by MŠMT under the grants no. LH11053 and 7E11017.

References

[1] D. A. Anisi and J. Thunberg, *Survey of patrolling algorithms for surveillance UGVs*. Swedish Defence Research Agency, April 2007.

[2] F. Capezio, A. Sgorbissa, and R. Zaccaria, "GPS-based localization for a surveillance UGV in outdoor areas," in *the Fifth International Workshop on Robot Motion and Control*, june 2005, pp. 157 – 162.

[3] C. C. Haddal and J. Gertler, "Homeland security : Unmanned aerial vehicles and border surveillance," *Aviation*, pp. 1–6, 2010.

[4] T. Krajník, V. Vonásek, D. Fišer, and J. Faigl, "AR-Drone as a Robotic Platform for Research and Education," in *International Conference on Research and Education in Robotics*. Prague: Springer, 2011.

[5] S. Lange, N. Sünderhauf, and P. Protzel, "A vision based onboard approach for landing and position control of an autonomous multirotor UAV in GPS-denied environments," *Electrical Engineering*, 2009.

[6] M. Bošnak, D. Matko, and S. Blažič, "Quadrocopter hovering using position-estimation information from inertial sensors and a high-delay video system," *Journal of Intelligent & Robotic Systems*, pp. 1–18, Dec. 2011. [Online]. Available: http://dx.doi.org/10.1007/s10846-011-9646-5

[7] T. Krajník et al., "Simple, yet Stable Bearing-only Navigation," *Journal of Field Robotics*, October 2010.

[8] N. Cornelis and L. Van Gool, "Fast scale invariant feature detection and matching on programmable graphics hardware," in *CVPR 2008 Workshop (June 27th)*, Anchorage Alaska, June 2008.

[9] H. Bay, A. Ess, T. Tuytelaars, and L. Van Gool, "Speeded-up robust features (SURF)," *Computer Vision and Image Understanding*, vol. 110, no. 3, pp. 346–359, 2008.

[10] T. Vintr et al., "Batch FCM with volume prototypes for clustering high-dimensional datasets with large number of clusters," in *World Congress on Nature and Biologically Inspired Computing*, 2011, pp. 427–432.

[11] T. Vintr, L. Pastorek, and H. Rezankova, "Autonomous robot navigation based on clustering across images," in *International Conference on Research and Education in Robotics*, Prague, 2011, pp. 310–320.

[12] P. J. Bristeau, F. Callou, D. Vissiere, and N. Petit, "The navigation and control technology inside the AR.Drone micro UAV," in *18th IFAC World Congress*, Milano, Italy, 2011, pp. 1477–1484.

[13] "Parrot AR Drone," http://ardrone.parrot.com, citied July 2011.

[14] "A video from UAV-UGV autonomous inspection." [Online]. Available: http://www.youtube.com/watch?v=RPCUB6xjQTI